

EXPERIMENTAL AND COMPUTER ANALYSES OF IMPACT PENETRATION OF A STEEL ROD INTO HEAVY PLATES OF STEEL AND ALUMINUM ALLOYS

L. Kruszk a⁽¹⁾,
G. V. Stepanov⁽²⁾, V. V. Kharchenko⁽²⁾, V. I. Zubov⁽²⁾

⁽¹⁾ **Military University of Technology,**
Warsaw, Poland

⁽²⁾ **National Ukrainian Academy of Sciences,**
Kiev, Ukraine

In the paper some results of experimental and numerical analysis concerning penetration of a steel rod (with conical and flat-faced heads) into heavy high-strength steel and AMg6, Al-Zn-Mg and D16 aluminum alloys plates are presented. The calculations are conducted for relatively low velocities of penetration (200–1000 m/s), so the hydrodynamic component of the pressure on the contact surface is much lower than the strength of the material with allowance for viscosity effects. In most variants, the strains in the rod are assumed to be elastic for revealing effects of viscosity of the plate material. The resistance to penetration at its initial stages (prior to the rod plastic flow and fracture) is found to be determined by the dynamic strength of the plate material, its viscous component (proportional to the plastic strain rate) prevailing at the impact velocities of up to 500 m/s. From the experimental analysis it follows that the depth of penetration varies with the velocity, and it is conditioned by wave processes in the plate, their scale being dependent on its thickness. Such experimental results are in agreement with results of computer simulation of the initial stage of rigid rod penetration in plates of limited thickness.

1. INTRODUCTION

The effect of strength and viscosity of the plate material on its resistance against rod penetration were discussed in many papers [1–4]. As an example, there are some data on the tungsten rod penetration into heavy steel plate at velocities of up to 1500 m/s [1]. According to experimental data, the depth of penetration into a plate made of steel of high strength RHA (homogeneous steel armor) is lower than into the plate of steel 4340 of lower strength. However, the influence of strength parameters of the plate material (yield stress, strain hardening, viscosity effects and other) on its resistance to penetration remains insufficiently investigated [5].

The penetration of a steel rod into an aluminum alloy plate is a complex process revealing major features of the material plastic flow at high strain rates. The computer simulation of such a process with the use of a nonlinear viscoelastoplastic model of the material can be used to evaluate the influence of high strain rate on its resistance to penetration, but practical application of these models remains difficult. Therefore the development of simplified engineering models of the rod-plate interaction and the estimation of the relationship between the process parameters and physical-mechanical characteristics of the material are still of interest. Such results are useful for revealing the influence of high strain rates and other peculiarities of plastic flow on the resistance to penetration of rods into plates of limited thickness.

The assumptions used in engineering models accounting for the effects of strength on the penetration process can be validated with the help of numerical simulation. For elimination of some effects masking the influence of strength, in the majority of published results, the velocity of steel rod varied in the range from 200 to 1000 m/s and plastic strains in this rod were neglected.

The analyses of experimental results obtained at penetration of steel rods into aluminum plates of different strength and thickness is here presented. The influence of viscosity effects on the penetration process is also investigated in this paper using computer simulation.

2. EXPERIMENTAL ANALYSIS

We have analyzed the results [6], obtained in experiments concerning penetration of a flat-faced steel rod of diameter $d = 14.5$ mm, and of length $l = 50$ mm, into AMg6 soft aluminum alloy plates of thickness $B = 30$ mm and 60 mm, or into Al-Zn-Mg hard aluminum alloy plate of thickness $B = 30$ mm. Two segments with a corner point represent the penetration curve $L(V)$ - Fig. 1. In all

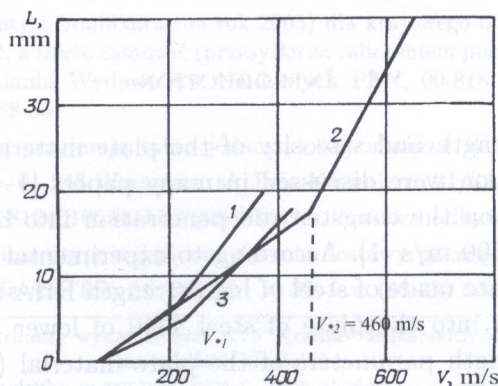


FIG. 1. Steel rod penetration depth L vs impact velocity V : 1 - AMg6 alloy, $B = 30$ mm; 2 - AMg6 alloy, $B = 60$ mm; 3 - Al-Zn-Mg alloy, $B = 30$ mm.

experiments, the penetration started at the velocity $V_0 \approx 70$ m/s. In the range of velocities from $V_0 = 70$ m/s to the value at the corner point V_* (for AMg6 alloy plate of $B = 30$ mm: $V_{*1} = 220$ m/s and $L = 7$ mm, of $B = 60$ mm $V_{*2} = 460$ m/s and $L = 17.5$ mm), the penetration depth L grows linearly with velocity; the linear segments exhibit the same slope. The thickness of a loaded plate does not influence the value V_0 and the above slope; for a thicker plate, the slope behind the corner point is steeper. For an Al-Zn-Mg alloy plate of higher strength ($B = 30$ mm, $V_* = 240$ m/s and $L = 5$ mm), the slope of the first segment is lower than that for the AMg6 plate.

Let us now analyze the above data using the concept of wave effects in loaded plates. When $V < V_0$, at the initial moment of interaction a plane wave with the stress amplitude at the front is initiated near the rod-plate contact surface:

$$(2.1) \quad \sigma_r = (\rho a)_1 V / [1 + (\rho a)_2 / (\rho a)_1],$$

where ρ and a are the density and the velocity of a longitudinal wave; indices 1 and 2 refer to the rod and the plate materials, respectively. If $V = V_0$, this stress is close to the Hugoniot elastic limit, i.e. pressure on the contact surface for one-dimensional strain state in the elastic plane wave. Assuming $\rho = 7800$ kg/m³, $a = 5000$ m/s for steel rod, and $\rho = 2800$ kg/m³, $a = 6000$ m/s for aluminum alloy at $V_0 = 70$ m/s, the Hugoniot elastic limit for the alloy is $\sigma_G = 830$ MPa. As the wave propagates into the plate, the stress amplitude at the elastic wave front decreases with a simultaneous change of the stress state, and change of the ratio of stress tensor components behind this front. At higher velocities $V > V_0$, essentially inelastic strain effects appear in the plate. Plastic strains in the rod made of the material with higher yield strength can be neglected. This causes the formation of a cone in aluminum plate adjoining the rod face. If this cone remains unchanged, its resistance to penetration is determined by the plastic flow around this cone head.

The corner point V_* on the penetration curve cannot be connected with wave processes in the rod, since the curve $L(V)$ varies with the thickness of a loaded plate. Thus, this corner point can be only a result of an abrupt change of the stress state caused by wave processes in the plate. This point is associated with the effect of a loading wave (coming from the rod-plate interface) reflected from the free back surface on the stress-strain state near the cone head. Since the penetration rate of the rod head is determined by its deceleration, connected with the stress field in the plate near the contact surface, an unloading wave affects this rate. Assuming that the corner point on the curve $L(V)$ is associated with the effect of the reflected wave, let us analyze the experimental penetration data for plates of thickness 30 mm and 60 mm corresponding to the area near the corner point. These data in the range of velocities $V_0 < V < V_*$ are described by the linear relationship

$$(2.2) \quad L(V) = \kappa(V - V_0),$$

where the coefficient κ for the first linear segment does not depend on thickness of the plate. In accordance with the above assumption, relationship (2.2) is valid until an intense unloading wave, reflected from the back surface of the plate, reaches the contact surface. When the plate thickness changes, the penetration depth corresponding to the corner point varies with the time of penetration prior to the arrival of the reflected wave.

According to the known literature data, a loading wave with a front similar to the spherical one propagates from the contact surface of the rod into the plate, its intensity decreasing by the ratio $(r_c/r)^\alpha$ (r_c , are the radii of the loaded spherical cavity and of the wave front, parameter $\alpha > 1$). Therefore the small effect of the first wave reflected from the free surface on the stress-strain state near the contact surface cannot sharply change this state, but after its repeated reflection and development of plastic strain, the stress-strain state becomes essentially different from the initial one, i. e. without the influence of the reflected wave effects. Let us assume that an abrupt change of the stress-strain state near the contact surface corresponding to the corner point V_* is connected with the effect of the front of an intense unloading wave after its repeated reflection from the free surface. When the plate thickness changes, the intensity of the unloading wave coming to the contact surface is maintained due to the corresponding increase in the initial wave intensity, i.e. due to a higher impact velocity proportional to the plate thickness. Thus, for the plate of thickness B_2 , the impact velocity $V_{*2} = V_{*1}(B_2/B_1)$ corresponds to the corner point. Taking into account that $\kappa = L_*(V_* - V_0)$, the penetration depth L_{*2} at the velocity V_{*2} is obtained:

$$(2.3) \quad L_{*2} = \kappa(V_{*2} - V_0) = L_{*1}(V_{*2} - V_0)/(V_{*1} - V_0).$$

Using data for penetration into the AMg6 plate of thickness 30 mm: $L_{*1} = 7.0$ mm, $V_{*1} = 220$ m/s, $V_0 = 70$ m/s and $V_{*2} = 460$ m/s, the calculated depth of penetration into the plate of thickness 60 mm: $L_{*2} = 7.0 \cdot (460 - 70)/(220 - 70) \approx 18.2$ mm, corresponding to the corner point, is in a fairly good agreement with experimental data - Table 1.

Table 1. Experimental and calculated data for characteristic points on the penetration curve for AMg6 plate.

Experiment			Calculation	
V , m/s	L , mm	B , mm	L/B	$(l/B)(V/V_* - 1)$
220	7.0	30	0.233	3.571
380	20.0	30	0.667	7.380
460	18.2	60	0.303	4.640
575	30.0	60	0.500	6.012

The intensity of the stress-strain state near the contact surface, caused by the influence of the unloading wave, varies continuously at impact velocities at $V > V_*$. In this case, the resistance to penetration is determined by the stress-strain state in the plate near the contact surface as a result of the direct effect of the rod penetration and the reflected unloading wave. The latter one causes non-uniform three-dimensional tension, which contributes to further penetration of the rod and makes the penetration curve steeper after the corner point. At higher plate thickness, where radius of the spherical unloading wave front is larger, wave effects are less effective on the resistance of the rod to penetration at the same depth.

Reduced penetration depth, corresponding to the intersection point, is obtained at rod penetration into a plate of harder alloy (with a higher strength) without essential change of line segment in the curve $L(V)$ inclination. Slight change of the penetration rate for soft and hard aluminum alloys can be attributed to the difference in wave velocities and parameters determining the kinetics of the material flow.

On the basis of experimental relation (2.2), the change of the rod momentum for $V_0 > V > V_*$ is equal to

$$(2.4) \quad \delta(mV) = P\delta t = (mV/\kappa)\delta t,$$

where m is the mass of the rod. Hence the longitudinal load on the interface at penetration $P = mV/\kappa$ is proportional to the penetration rate V . The middle pressure on the rod head, with the static H_s , viscous $H_v = \mu\epsilon'$ and hydrodynamic $H_g = \rho V^2/2$ components taken into account

$$(2.5) \quad p = (\rho l)_r V/\kappa = H_s + \mu\epsilon' + \rho_2 V^2/2 \approx \mu\epsilon'$$

reaches the value $p \approx 3.87$ GPa near the corner point $V_{*2} = 460$ m/s at penetration into AMg6 aluminum alloy, taking the length of steel rod $l = 0.05$ m and $\kappa^{-1} = (460 - 70)/0.0182 = 21400$ s⁻¹. In the above listed experiments, the maximum value of hydrodynamic pressure on the rod at stable penetration in aluminum alloy, assuming that $V < 460$ m/s, $\rho_p = 2800$ kg/m³: $\rho_p V^2/2 < 2800 \cdot 460^2/2 \approx 0.3$ GPa, and the static resistance (with the account of the adiabatic heating of the material) $H_s < 0.83$ GPa are relatively small, the viscous component of resistance corresponding to the experimental linear relation $L(V)$ prevails.

The characteristic strain rate of the material near the rod head is determined by its diameter $\epsilon' \approx 2V/d$. Therefore, the average value of the viscosity coefficient calculated from experimental data: $\mu = (\rho l)_r d/\kappa = (\rho l)_r (V_2 - V_*)d/(2L_2) = 7850 \cdot 0.050 \cdot 0.0145 (460 - 70)/(2 \cdot 0.0182) \approx 60000$ Pa·s, in the range of strain rates: $\epsilon' \approx 2V/d = 5000 \div 50000$ s⁻¹, is in good agreement with the known experimental

data [7]. The linear relation $L(V)$ points to the fact that over the rod velocity range under investigation, the effects of the viscous flow of the material prevail near the contact surface, despite a possible increase in temperature near this surface.

Using the above approach [7, 10], the penetration results in Fig. 1 can be represented in the dimensionless coordinates: $L/B - (l/B)(V/V_* - 1)$ as a single curve - Fig. 2. This confirms the accepted assumption of the influence of wave processes in the loaded plate, their scale being determined by the plate thickness, on the penetration depth.

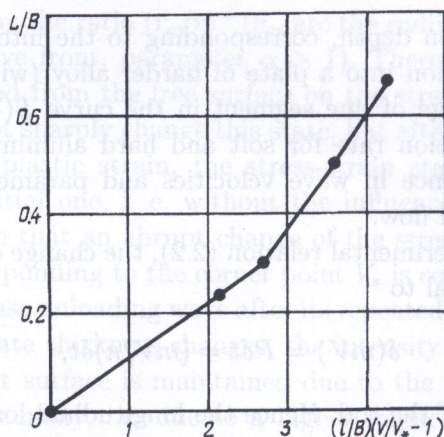


FIG. 2. Experimental penetration data in the dimensionless coordinates.

3. COMPUTATIONAL ANALYSIS

3.1. Equations of state of the plate material

Viscoplastic model of the material behavior under dynamic loading was used for numerical calculations. Plastic strain rate intensity ε'_p as the function of the overstress $\sigma_I - \sigma_{st}(\varepsilon_p)$ was calculated by the known Perzyna's equation:

$$(3.1) \quad \varepsilon'_p = \frac{\sigma_i - \sigma_{st}(\varepsilon_p)}{\mu(\varepsilon_p, \varepsilon'_p)}.$$

In this equation σ_i is the strain intensity and $\sigma_{st}(\varepsilon_p)$ is the stress under quasi-static loading with low strain rate ε'_0 as the function of plastic strain intensity ε_p .

Equation (3.1) for stress intensity is usually written in simple form with linear and nonlinear viscosity components of strength at plastic flow [9],

$$(3.2) \quad \sigma = \sigma_{st}(\varepsilon_p) + K(\varepsilon_p) \cdot \ln \left(\frac{\varepsilon'_p}{\varepsilon'_0} \right) + \mu \cdot \varepsilon'_p.$$

For simplification of the analysis of viscosity effects at penetration, most of the calculations were performed for a constant viscosity factor μ , the range of which corresponds to those determined experimentally in tests on structural materials, i.e. aluminum alloy D16 and high-strength steel [7, 8].

Stress-strain relation under quasi-static loading $\sigma_{st}(\varepsilon_p)$ used in calculations accounts for strain hardening as well as for softening (the latter can be essential at high strain rate and large strain due to their development in the material damage and to adiabatic increase of temperature during plastic flow):

$$(3.3) \quad \sigma_{st}(\varepsilon_p) = \sigma_Y(1 + A \cdot \varepsilon_i^n)(1 - B \cdot \varepsilon_i),$$

where σ_Y is the yield stress of the material under quasi-static loading.

3.2. Scheme of numerical calculations

Application of the program IMPRO based on triangular finite element code developed in the Institute of Problems of Strength, National Ukrainian Academy of Sciences [9], was used for computer simulations of two-dimensional axisymmetric penetration problems.

Plastic strain rate was calculated using the value of "overstress" according to the visco-plastic model of Perzyna with coefficient of viscosity appropriate to the experimental data for an aluminum alloy D16 and heavy high-strength steel. Two variants of impact interaction of a rod and steel plate were considered. These variants include penetration of a rigid (elastically non-deformable) rod with a conical head part (apex angle of 90°) and penetration of a plastically deformable

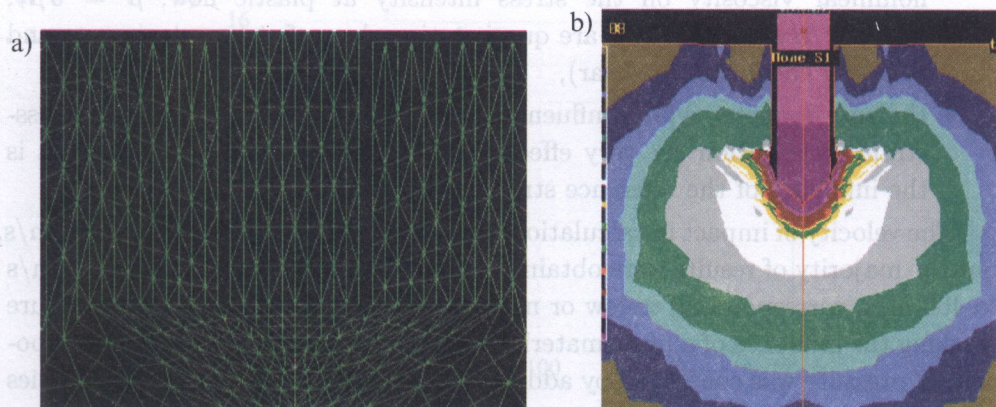


FIG. 3. Finite element grid (a) and contour lines of stress intensity σ_i (b) after 16 ms of penetration into thick aluminum alloy D16 plate ($\tau_Y = 400$ MPa, $A = 0$, $\mu_r = 10^4$ Pa·s with the initial hole of 25 mm depth) of the rigid rod (of 10 mm diameter with conical head, $V = 400$ m/s).

rod of the same geometry. Intense plastic flow in the plate (near the contact surface) causes large distortions of the grid, so transformed finite elements were used after a certain period of time. Calculations of a rod penetration into the face layer of the plate and into the bottom of the cylindrical cavity of 2.5-diameter depth (to eliminate the front face influence on stress-strain distribution in the plate near the contact surface) were conducted. The typical variant of a grid used for finite element code simulation of a steel rod penetration is shown in Fig. 3. Number of cells along the rod radius (usually equal to 5...7) enables adequate accuracy of such calculations.

3.3. Numerical results

Evaluations of the influence of strength effects on penetration were limited to penetration of a steel rod into heavy plates made of steel of different strength and high strength D16 aluminum alloy, with variable strain hardening/softening and variation of linear viscosity factor. More than 50 combinations of parameters material equations of state in the plate and various loading conditions were used in simulation of the rod penetration. The main variants presented in the paper include variation of:

- the yield stress of the plate material, strain hardening/softening, defined by the set of parameters \mathbf{A} , \mathbf{B} and \mathbf{n} in Eq. (3.3),
- parameters K, μ in the equation (3.2) defining the influence of linear and nonlinear viscosity on the stress intensity at plastic flow; $\mu = 3\mu_\tau$; $\mu_\tau = \partial\tau/\partial\gamma'_p$ (τ, γ' and μ are quasi-static values of stress, strain rate and viscosity coefficient in shear),
- the rod diameter which influences the maximum strain rate and stress-strain distribution are very effective and display the scale effects, that is the influence of the reference strain rate V/d .

The velocity of impact in calculations varied in the range from 200 to 1500 m/s, but the majority of results were obtained for velocities of the range from 200 m/s to 400 m/s, corresponding to low or negligible hydrodynamic (inertial) pressure masking the influence of a plate material strength. Significance of inertial component of pressure was confirmed by additional calculations with different densities of the plate material.

The distributions of stresses, strains and their rates ($\sigma_y, \sigma_i, \epsilon_i, \epsilon'_i$), loss of kinetic energy, deceleration of the rod, geometric form and extension of plastic flow area, were compared for different variants of calculations. Some results of calculation are shown in Fig. 4 a-d.

For the impact velocity of 400 m/s, the calculated strain rate intensity near the contact surface (in the middle of conical head) was about 10^4 s^{-1} for the rod diameter of $d = 10 \text{ mm}$ and about 10^5 s^{-1} for $d = 1 \text{ mm}$, so the strain rate is inversely proportional to the rod diameter. An increase of stresses along the rod axis up to a maximum level at the cone apex was obtained as a result of inhomogeneous stress state near the conical head of the rod. For plastically deformed rod, similar (but damped) increase of stresses follows from the calculations. In penetration of a cylindrical rod with conical head, the plastic flow corresponds to cylinder's symmetry for the material near the contact surface (near the conical head) and a spherical symmetry at some distance from it – see Fig. 3.

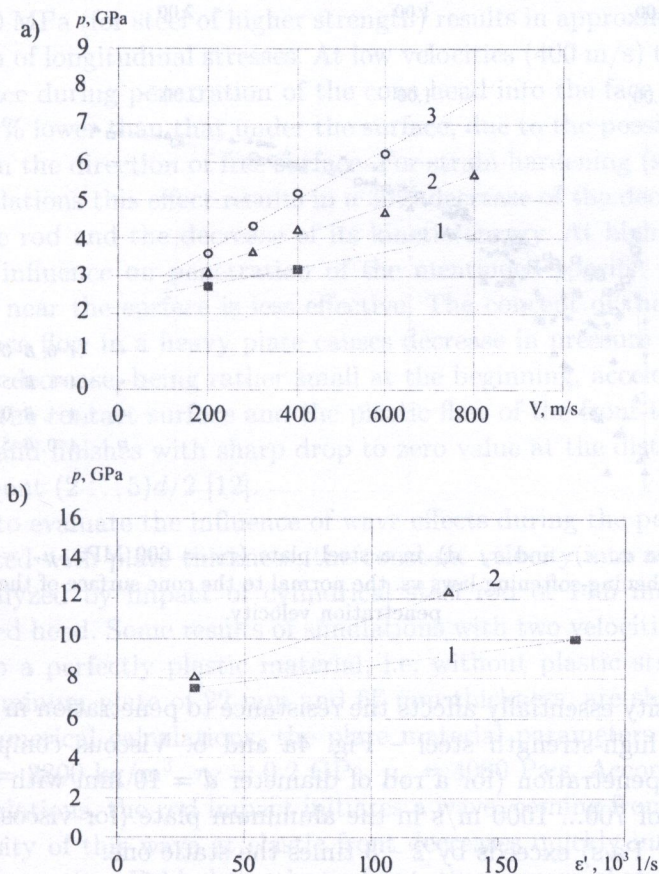


FIG. 4. a) Resistance to penetration (pressure p in the middle of conical head) of steel rod of 10 mm diameter in aluminum alloy D16 plate ($\tau_Y = 200 \text{ MPa}$, $A = 0$) with different viscosity factors: 1 – $\mu_\tau = 4 \cdot 10^3 \text{ Pa} \cdot \text{s}$ ($p = 0.0023 \cdot V + 2.3$); 2 – $\mu_\tau = 10^4 \text{ Pa} \cdot \text{s}$ ($p = 0.0041 \cdot V + 2.3944$); 3 – $\mu_\tau = 2 \cdot 10^4 \text{ Pa} \cdot \text{s}$ ($p = 0.0067 \cdot V + 2.3357$); b) Resistance to penetration of steel rod of 10 mm diameter in steel plate ($\tau_Y = 600 \text{ MPa}$, $A = 0$) with different viscosity factors: 1 – $\mu_\tau = 4 \cdot 10^3 \text{ Pa} \cdot \text{s}$ ($p = 0.0167 \cdot V + 7$); 2 – $\mu_\tau = 10^4 \text{ Pa} \cdot \text{s}$ ($p = 0.042 \cdot V + 6.84$).

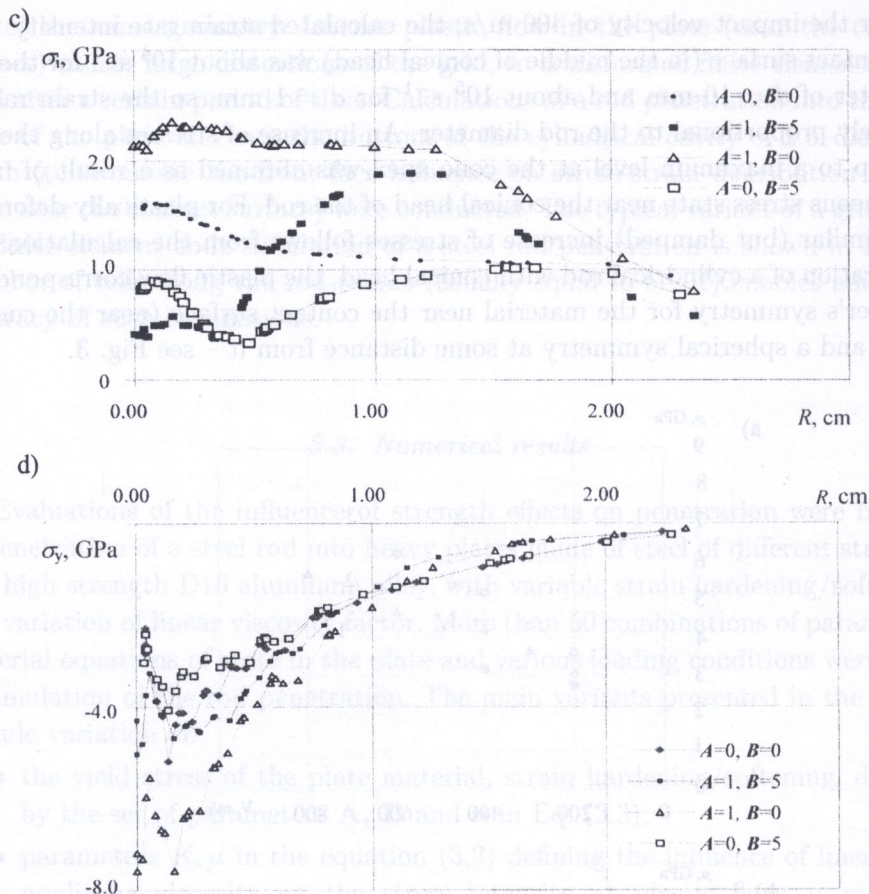


FIG. 4. Stresses σ_i c) and σ_y d) in a steel plate ($\tau_Y = 600$ MPa, $\mu_\tau = 10^4$ Pa·s) with different strengthening-softening laws vs. the normal to the cone surface of the rod at 400 m/s penetration velocity.

The viscosity essentially affects the resistance to penetration in an aluminum alloy and in high-strength steel – Fig. 4a and b. Viscous component of full resistance to penetration (for a rod of diameter $d = 10$ mm with conical head) at a velocity of 700... 1000 m/s in the aluminum plate (for viscosity coefficient of $\mu_\tau = 2 \cdot 10^4$ Pa·s) exceeds by 2 – 3 times the static one.

For high-strength steel ($\sigma_Y = 1000$ MPa, $\mu_\tau = 10^4$ Pa·s), in the above mentioned velocity range, the calculated resistance to penetration increases 1.5 times with 10-fold increase of the reference strain rate $\varepsilon_r = V/d$.

The effect of impact velocity on the resistance to penetration in plates of D16 aluminum alloy and high-strength steel obtained in computer simulation (for the viscosity coefficients of $\mu_\tau = 4 \cdot 10^3$, 10^4 and $2 \cdot 10^4$ Pa·s) was close to the

results obtained using engineering models of penetration [11], in which viscous component of pressure at the contact surface was determined from equations:

$$(3.4) \quad \sigma_{vs} = (4/3) \cdot \mu \cdot (V/d) \cdot \sin 2\alpha^*, \quad \varepsilon' = (V/d) \cdot \sin 2\alpha^*,$$

where $2\alpha^*$ is the apex angle of a cone head of the rod.

Strain hardening of the plate material does considerably increase the resistance to rod penetration (increases pressure at contact surface and strain intensity as shown in Fig. 4c and d. For the exponential strain hardening law ($\sigma = A \cdot \varepsilon_i^n$) the influence of the exponent value n is small due to large strains near the contact surface. The increase of constant A from 600 MPa (for mild steel) to 1000 MPa (for steel of higher strength) results in approximately proportional growth of longitudinal stresses. At low velocities (400 m/s) the pressure at contact surface during penetration of the cone head into the face layer of heavy plate was 20 % lower than that under the surface, due to the possibility of easier plastic flow in the direction of free surface. For strain hardening (softening) laws used in calculations this effect results in a 30% decrease of the deceleration force acting on the rod and the decrease of its kinetic energy. At higher penetration velocity the influence on penetration of the mentioned specific plastic flow of the material near the surface is less effective. The concept of the plastic front-to-back-surface flow in a heavy plate causes decrease in pressure at the contact surface. This decrease, being rather small at the beginning, accelerates with the approach of the contact surface and the plastic flow of the front-to-back-surface of the plate and finishes with sharp drop to zero value at the distance from this surface of about $(2 \dots 5)d/2$ [12].

In order to evaluate the influence of wave effects during the penetration process, connected with plate thickness, the constant velocity into aluminum plate end was analyzed by impact of cylindrical steel rod of 14.5 mm in diameter with flat-faced head. Some results of simulations with two velocities: 80 m/s and 140 m/s into a perfectly plastic material, i.e. without plastic strain hardening model of aluminum plate of 22 mm and 67 mm thickness, are shown in Fig. 5a and b. In numerical calculations, the plate material parameters used were the following: $\rho = 2800 \text{ kg/m}^3$, $\tau_Y = 0.2 \text{ GPa}$, $\mu_T = 4000 \text{ Pa}\cdot\text{s}$. According to the results of calculations, the rod impact initiates a wave, coming from the interface. Stress intensity of this wave at elastic front decreases quickly in the process of the wave propagation. Behind the elastic front, the increase of stress intensity to maximum value at the interface is obtained. After some time, the wave reflected from the back surface of plate propagates in opposite direction. The reflected wave effects on rod-plate interface becomes essential at later stages, being negligible at the beginning. These effects are clearly visible in distribution of velocity of the plate material near the axis of symmetry in different moments after ini-

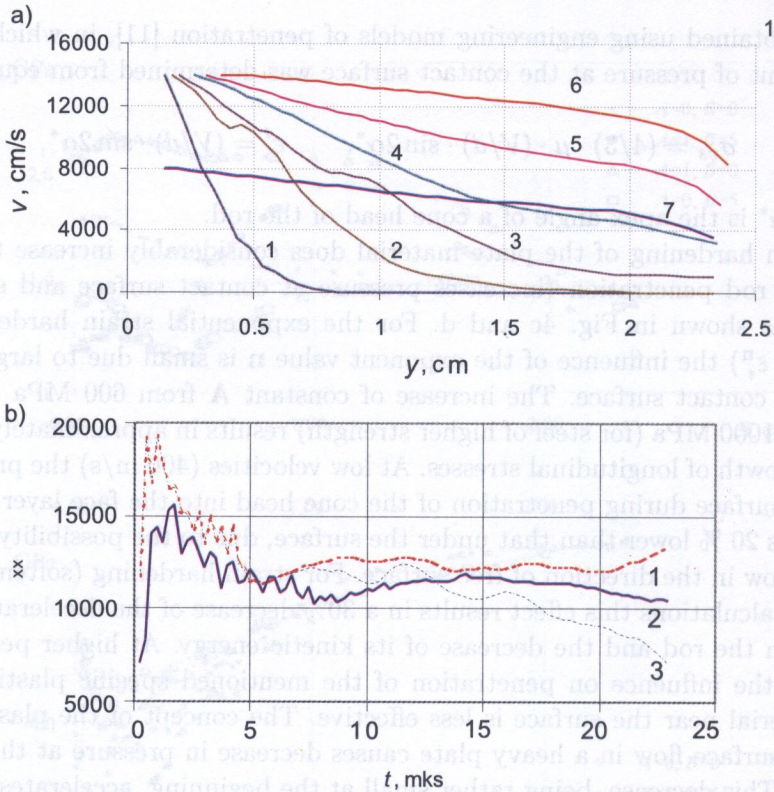


FIG. 5 a) Velocity in the AMg6 aluminum alloy plate ($B = 22$ mm) vs the axis of symmetry at penetration of the rod after various times of loading: 1...6 - ($t = 1, 3, 5, 9, 13, 17$ μ s; $V = 140$ m/s); 7 - ($t = 17$ μ s; $V = 80$ m/s); b) Pressure history of the stress $\sigma_{xx}(t)$ on the rod-plate interface near the axis of symmetry, at penetration of a rod into the AMg6 aluminum alloy plate: 1 - $B = 67$ mm, $V = 140$ m/s; 2 - $B = 22$ mm, $V = 80$ m/s; 3 - $B = 22$ mm, $V = 140$ m/s.

Pressure at the interface during penetration of the rod in a thick plate after a short period of time decreases to approximately constant value, associated with stationary stage of penetration - see curve 1 in Fig. 5a. The pressure near the axis of symmetry in this stage of penetration equals approximately 1.2 GPa, exceeds 3.46 times the material strength obtained during static loading $Y = 0.35$ GPa and used in calculations. In a thin plate, which a visible decrease of interface pressure with time is obtained after the time period from the initiation of loading exceeds the time necessary for arrival of the reflected wave front. So, this decrease in pressure is connected with later stages of waves interactions.

The decrease of penetration velocity used in calculation leads to higher pressure on the interface, connected with smaller influence of the reflected wave of lower intensity. This follows from comparison of curves 2 and 3 in Fig. 5b. The influence of viscosity effects leads to the increase of pressure at the contact sur-

lower intensity. This follows from comparison of curves 2 and 3 in Fig. 5b. The influence of viscosity effects leads to the increase of pressure at the contact surface after the initial period of unstable stress-strain state in the material near the contact surface.

4. CONCLUSIONS

The penetration data, obtained at impact of a steel rod into aluminum thick plates, allow to conclude that the resistance to penetration at small velocities (that disable the rod plastic flow and fracture) is determined by the dynamic strength of the plate, its viscous component (proportional to the plastic strain rate) prevailing at impact velocities of up to 500 m/s. The penetration depth of the rod into the aluminum thick plate varying with the velocity is essentially affected by wave processes in the plate, their scale being dependent on the thickness and strength of the plate. Experimental results are in agreement with computer simulation of the initial stage of penetration results, showing the influence of wave effects in the plate on the pressure at contact surface.

From the results of computer simulation it follows that the effects of viscosity are essential for penetration into surface layer of the plate as well as into inner layers. At a penetration velocity of 400 m/s, the strain rate near the contact surface of about 10^4 1/s for the rod diameter of 10 mm with conical head follows from calculation. For a rod diameter of 1.0 mm, a higher strain rate (about 10^5 s⁻¹) was calculated, revealing essential result of the scale effect. Stress distribution along the conical head of the rod, deformed elastically, reaches its maximum value at some distance from the contact surface near the cone apex. Similar effect is obtained in the case of small plastic strain developing in the rod. Plastic flow in a plate material near the contact surface with the conical head corresponds with good accuracy to cylinder symmetry. At some distance from this surface, the plastic flow can be approximated by spherical symmetry. Viscosity component of full resistance to penetration of a rigid rod (in the velocity range from 700 to 1000 m/s) penetrating into heavy plate exceeds the quasi-static component of plate strength material by 1.5 – 3 times.

ACKNOWLEDGMENTS

Gratitude is expressed to the State Committee for Scientific Research (Poland) for financial support under Grant No. 0T00A 017 15.

REFERENCES

1. A. M. RAJENDRAN, *Penetration of tungsten alloy into shallow-cavity steel targets*, Int. J. Impact Engng., 6, 21, 451–460, 1998.

2. R. C., BATRA *Steady state penetration of thermoviscoplastic targets*, Computational Mechanics, 1, 3, 1–12, 1998.
3. C. E. ANDERSON, S. A. MULLIN, C. J. KUHLMAN, *Computer simulation of strain-rate effects in replica scale model penetration experiments*, Int. J. Impact Engng., 1, 13, 35–52, 1993.
4. M. J. FORRESTAL, and V. K. LUK, *Dynamic spherical cavity-expansion in a compressible elastic-plastic solid*, J. Appl. Mech., 55, 2, 275–279, 1988.
5. G. V. STEPANOV and V. V. KHARCHENKO, *The influence of dynamic material behavior on long rod penetration at elevated velocities*, Problems of Strength, 4, 39–51, 1998.
6. V. V. ASTANIN, SH. U. GALEV and K. B. IVASHCHENKO, *Specific features of deformation and fracture of aluminum targets interacting with a steel penetrator along the normal*, Probl. Prochn., 12, 52–58, 1988.
7. G. V. STEPANOV, *Elastic-plastic deformation and fracture of materials under impulsive loading* (in Russian), Naukova Dumka, Kiev 1991.
8. G. V. STEPANOV, V. I. ZUBOV, *High-rate dynamic compression of high-strength steel and titanium alloy* (in Ukrainian), [in:] Naukovi Visti, NTUU “KPI”, 6, 76–81, 2000.
9. V. V. KHARCHENKO, *Simulation of high strain-rate of metals with account of viscoplastic effects* (in Russian), LOGOS, Kiev 1999.
10. G. V. STEPANOV, A. A. AVETOV, A. M. ULCHENKO, *Impulse of forces at rupture of targets with a steel penetrator*, Probl. Prochn., 9, 57–59, 1986.
11. V. V. KHARCHENKO, *Rigid rod penetration in viscoplastic media* [in Russian], [in:] Dynamic Strength and Fracture Toughness of Structural Materials, 52–56, Kiev 1989.
12. G. V. STEPANOV, V. V. KHARCHENKO L. KRUSZKA, *Analysis of the aluminum alloy resistance to the penetration of a steel rod at velocities up to 500 m/s*, Proceedings of the XV International Scientific-Technological Conference on Environmental Engineering in Maintenance of Military Complexes, 10–12 October, Military University of Technology, 2, 372–380, Zakopane 2001.

Received July 5, 2004; revised version February 12, 2004.